J|A|C|S
COMMUNICATIONS

Published on Web 03/03/2006

Biocleavable Polyrotaxane−Plasmid DNA Polyplex for Enhanced Gene Delivery

Tooru Ooya,[†] Hak Soo Choi,[†] Atsushi Yamashita,[†] Nobuhiko Yui,*[,†] Yuko Sugaya,[‡] Arihiro Kano,[‡] Atsushi Maruyama,*[,‡] Hidetaka Akita,[§] Rie Ito,[§] Kentaro Kogure,[§] and Hideyoshi Harashima*[,§]

School of Materials Science and the 21st COE Program, Japan Advanced Institute of Science and Technology, 1-1 Asahidai, Nomi, Ishikawa 923-1292, Japan, Institute of Materials and Chemical Engineering, Kyushu University, Hakozaki, Fukuoka 812-8581, Japan, and Graduate School of Pharmaceutical Sciences, Hokkaido University, Kita 12, Nishi 6, Sapporo 060-0812, Japan

Received August 26, 2005; E-mail: yui@jaist.ac.jp

Gene delivery using cationic polymers is one of the greatest challenges for inventing nonviral gene carrier systems instead of toxic virus-based vector systems.[1] High-molecular-weight polycations, such as polyethyleneimine, have been studied as a nonviral gene vector that effectively condenses plasmid DNA (pDNA) to prepare a stable polyplex,[1d,f] whereas low-molecular-weight polycations are much more advantageous in terms of decondensation of the polyplex as well as high transfection and low cytotoxicity.[1d] Introducing many disulfide linkages into the main chain of polycations has been reported as a key for controlling intracellular gene delivery[2] because the pDNA polyplex is decondensed in cytosolic milieu via cleavage of disulfide linkages.[2b] However, gene transfer efficiency in relation to endosomal escape decreases with increasing the number of disulfide linkages due to over stabilization of the polyplex, resulting in insufficient cleavage.[3] In this point of view, we designed a biocleavable polyrotaxane (Scheme 1a) that has a necklace-like structure[4] between many cationic α-cyclodextrins (α-CDs) and a disulfide-introduced poly(ethylene glycol) (PEG). It is expected that the polyrotaxane shows sufficient cleavage of disulfide linkages under reducible conditions because only two disulfide linkages can avoid the over stabilization. The cleavage will lead to triggering pDNA decondensation (pDNA release) via the dissociation of the noncovalent linkages between α-CDs and PEG, looking like a necklace in pieces (Scheme 1b). Here, we report a critical role of the polyrotaxane polyplex and supramolecular dissociation of the biocleavable polyrotaxane to its building blocks for endosomal escape and pDNA delivery to the nucleus.

Scheme 1. Chemical Structure of Biocleavable Polyrotaxane (a), Image of the Polyplex Formation and Terminal Cleavage-Triggered Decondensation of the Polyplex (b)

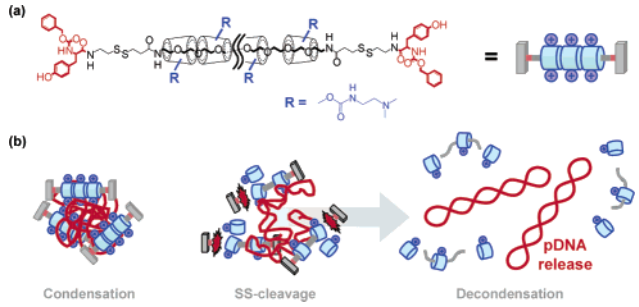

We synthesized the biocleavable polyrotaxane, in which dimethylaminoethyl-modified α-CDs (DMAE-α-CDs) are threaded onto a PEG (M_n = 4000) chain capped with benzyloxycarbonyl tyrosine via disulfide linkages that exist only at both termini of the PEG chain (DMAE−SS−PRX). From the ^{1}H NMR spectra, the number of threading α-CDs and DMAE groups per polyrotaxane was calculated to be ca. 23−30[5] and 40, respectively. On a MALS-GPC chart, the DMAE−SS−PRX showed one peak with shorter retention time than DMAE-α-CDs.[6] These results indicate that free DMAE-α-CDs were not contaminated in the DMAE−SS−PRX.

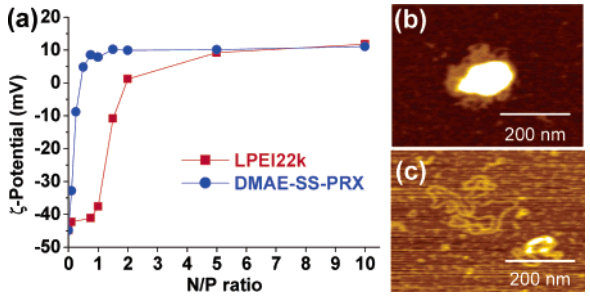

Figure 1. (a) ζ-Potentials of the DMAE−SS−PRX polyplex (blue line) and the LPEI22k polyplex (red line). AFM image of the pDNA polyplex with the DMAE−SS−PRX (b) and LPEI22k (c) at N/P = 0.5.

The pDNA complexation of the DMAE−SS−PRX was compared with a linear polyethyleneimine with M_n of 22 000 (LPEI22k) in terms of agarose gel electrophoresis and ζ-potentials. When the DMAE−SS−PRX was mixed with the pDNA, the free pDNA band on the gel electrophoresis image disappeared above the N/P ratio of 0.5. On the other hand, the DMAE-α-CD, one of the building blocks of the DMAE−SS−PRX, did not form any polyplexes at wide N/P ratios. These results indicate that the polycationic nature of the DMAE−SS−PRX contributes to stable polyplex formation. The ζ-potential of the DMAE−SS−PRX polyplexes at the N/P ratio of 0.5 was +4.8 mV (Figure 1a), and the DMAE−SS−PRX formed a tightly packed pDNA polyplex (Figure 1b), the diameter of which was around 178−189 nm determined by a dynamic light scattering measurement. On the contrary, LPEI22k did not form any tightly packed polyplex at the same N/P ratio (Figure 1c). The ζ-potential of the DMAE−SS−PRX polyplexes became positive when the N/P ratio was 0.25−0.5, although the LPEI22k polyplex still showed a negative value. These data suggest that the DMAE−SS−PRX can condense pDNA more efficiently than LPEI22k even at a low charge ratio. Furthermore, pK_a of the DMAE−SS−PRX and LPEI22k was 7.5 and 8.0, respectively.[6] This means that only half of the DMAE groups was protonated and contributed to the pDNA complexation in the buffer (pH 7.4). Therefore, the driving force of the pDNA condensation of the DMAE−SS−PRX should be not only electrostatic interaction but also the other factors of polyrotaxane structure, such as rod-like structure and association of the terminal benzyloxycarbonyl group.[7] In addition, the mobile motion of α-CDs in the necklace-like structure[8] of the DMAE−SS−PRX might prevent spatial mismatching in multivalent interaction

[†] Japan Advanced Institute of Science and Technology.
[‡] Kyushu University.
[§] Hokkaido University.

10.1021/ja055868+ CCC: $33.50

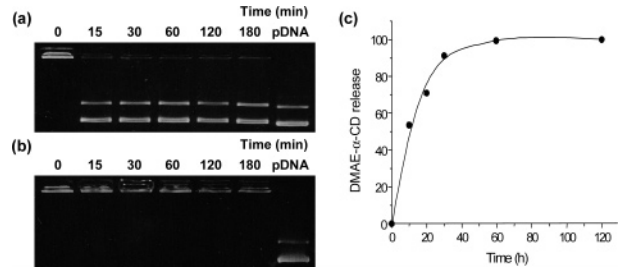

Figure 2. Agarose gel electrophoresis data of pDNA release from the polyplex with the DMAE−SS−PRX (a) and the DMAE-PRX (b) (N/P = 5) in the presence of 10 mM DTT and dextran sulfate (M_n = 25 000) as a counter polyanion. DMAE-α-CD release from the DMAE−SS−PRX in the presence of 10 mM DTT (c).

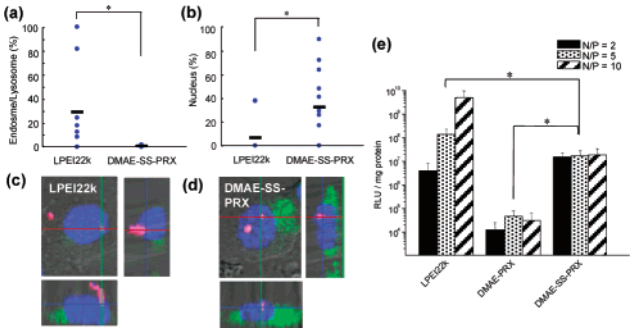

Figure 3. Comparison of the endosome/lysosome (a) and the nucleus (b) distributions of pDNA transfected with DMAE−SS−PRX and LPEI22k at N/P = 5.[9] At 90 min after transfection, the fractions of the pDNA in endosome/lysosome were quantified. Black bars represent the mean values (n = 10). Asterisks indicate significant differences between two polymers, determined by the Mann−Whitney test (P < 0.05). CLSM images for the LPEI22k (c) and the DMAE−SS−PRX (d) polyplexes (N/P = 5) after 90 min transfections were shown below the quantified graph. Endosome/lysosome (green) was stained by Lysosensor, and the blue fluorescence shows the Hoechst 33258-stained nuclei. The rhodamine-labeled pDNA shows a red fluorescence. Transfection efficiency with the DMAE−SS−PRX, DMAE-PRX, and LPEI22k (n = 7−9) (e). Asterisks indicate significant differences between two polymers at each N/P ratio, determined by the Welch test (P < 0.05).

between the cationic groups and anionic groups in pDNA, resulting in the effective condensation of pDNA.

In vitro pDNA decondensation experiments in the presence of 10 mM dithiothreitol (DTT) confirmed that pDNA was released from the DMAE−SS−PRX polyplex in the presence of counter polyanion (Figure 2a). However, the polyplex of DMAE-introduced polyrotaxane (DMAE−PRX), which has no disulfide linkages, was stable in the same condition (Figure 2b). Since the DMAE-α-CDs were released in the same reducible condition (Figure 2c), the disulfide cleavage under the reducible condition led to unstable polyplex via PEG dethreading from DMAE-α-CD cavities, and interexchange with polyanions decondensed the unstable polyplex.

The positively charged surface of polyplex and supramolecular dissociation of the DMAE−SS−PRX is expected to improve the intracellular trafficking and transfection efficiency. The intracellular trafficking was evaluated by quantitative three-dimensional analysis using confocal laser scanning microscopy (CLSM) technique.[9] Surprisingly, the DMAE−SS−PRX polyplex (N/P = 5) completely escaped from the endosome and/or lysosome (endosome/lysosome) 90 min after transfection (Figure 3a). Presumably, much more positively charged surface of the DMAE−SS−PRX polyplex (Figure 1a) than the LPEI22k polyplex and the good buffering capacity[6] are advantageous to show the proton sponge effect. It was noted that about 30% of pDNA cluster was found to be located in the nucleus, being clearly confirmed by the CLSM image as pink-colored spots (Figure 3b,d). In the case of the LPEI22k polyplex, pDNA cluster seems to be located above the nucleus (Figure 3c), and 30% of pDNA was still located in the endosome/lysosome even at the same incubation time (Figure 3a). Therefore, high localization of pDNA cluster in the nucleus is due to rapid endosomal escape of the DMAE−SS−PRX polyplex. Further, the DMAE−SS−PRX polyplex affected the transfection efficiency. The transfection efficiency of the DMAE−SS−PRX polyplex was independent of the N/P ratio, although that of the LPEI polyplex was apparently dependent on the N/P ratio (Figure 3e). These results suggest that the transfection of the DMAE−SS−PRX polyplex is independent of the amount of free polycation. Since the transfection efficacy of the DMAE−SS−PRX polyplex was much higher than that of the DMAE−PRX, the disulfide cleavage played a key role in the gene expression.

In conclusion, a stable polyplex with positively charged surface was formed by mixing very small amounts of the DMAE−SS−PRX with pDNA, which is likely to be due to the mobile motion of α-CDs in the necklace-like structure of the DMAE−SS−PRX. The pDNA decondensation of the polyplex occurred through disulfide cleavage of the DMAE−SS−PRX and subsequent interexchange with polyanions. Rapid endosomal escape and pDNA delivery to the nucleus were achieved by the polyplex. This work, with further suitable design of the DMAE−SS−PRX, allows the development of nonviral gene delivery and may be particularly important for synthetic biomaterials design used for beneficial gene therapy.[1a]

Acknowledgment. We acknowledge Mr. Atsuto Yoshihiro, JAIST, for helping with this study. This work was financially supported by a Grant-in-Aid for Scientific Research (B) (No. 14380397), and JAIST 21st Century COE Program "Scientific Knowledge Creation Based on Knowledge Science".

Supporting Information Available: Experimental methods, synthetic procedure, GPC charts, agarose gel electrophoretic images, titration, CLSM image, and cells viability. This material is available free of charge via the Internet at http://pubs.acs.org.

References

(1) (a) Wolff, J. A. *Nat. Biotechnol.* **2002**, *20*, 768−769. (b) Han, S.-O.; Mahato, R. I.; Sung, Y. K.; Kim, S. W. *Mol. Ther.* **2000**, *2*, 302−317. (c) Nori, A.; Kopeček, J. *Adv. Drug Delivery Rev.* **2005**, *57*, 609−639. (d) Kunath, K.; Harpe, A.; Fischer, D.; Petersen, H.; Bickel, U.; Voigt, K.; Kissel, T. *J. Controlled Release* **2003**, *89*, 113−125. (e) Fukushima, S.; Miyata, K.; Nishiyama, N.; Kanayama, N.; Yamasaki, Y.; Kataoka, K. *J. Am. Chem. Soc.* **2005**, *127*, 2810−2811. (f) Kong, H. J.; Liu, J.; Riddle, K.; Matsumoto, T.; Leach, K.; Mooney, D. J. *Nat. Mater.* **2005**, *4*, 460−464.

(2) (a) Saito, G.; Swanson, J.; Lee, K.-D. *Adv. Drug Delivery Rev.* **2003**, *55*, 199−215. (b) Read, M. L.; Bremner, K.; Oupicky, H.; Green, N. K.; Searle, P. F.; Seymour, L. W. *J. Gene Med.* **2003**, *5*, 232−245. (c) Gosselin, M. A.; Guo, W.; Lee, R. J. *Bioconjugate Chem.* **2001**, *12*, 989−994. (d) Miyata, K.; Kakizawa, Y.; Nishiyama, N.; Harada, A.; Yamasaki, Y.; Koyama, H.; Kataoka, K. *J. Am. Chem. Soc.* **2004**, *126*, 2355−2361.

(3) Oupicky, D.; Carlisle, R. C.; Seymour, L. W. *Gene Ther.* **2001**, *8*, 713−724.

(4) (a) Harada, A.; Li, J.; Kamachi, M. *Nature* **1992**, *356*, 325−328. (b) Shigekawa, H.; Miyake, K.; Sumaoka, J.; Harada, A.; Komiyama, M. *J. Am. Chem. Soc.* **2000**, *122*, 5411−5412. (c) Ooya, T.; Yui, N. *Crit. Rev. Ther. Drug Carrier Syst.* **1999**, *16*, 289−330. (d) Ooya, T.; Eguchi, M.; Yui, N. *Biomacromolecules* **2001**, *2*, 200−203.

(5) The number of α-CDs of 23 corresponds to 51% threading onto the PEG chain. Stoichiometric number of α-CDs is ca. 45, assuming that two ethylene glycol units are included in one α-CD molecule.

(6) See Supporting Information.

(7) Ooya, T.; Yui, N. *Macromol. Chem. Phys.* **1998**, *199*, 2311−2320.

(8) (a) Ooya, T.; Eguchi, M.; Yui, N. *J. Am. Chem. Soc.* **2003**, *125*, 13016−13017. (b) Ooya, T.; Utsunomiya, T.; Eguchi, M.; Yui, N. *Bioconjugate Chem.* **2005**, *16*, 62−69.

(9) Total pixel area of rhodamine-labeled pDNA in whole cell ($S_{(tot)}$) and each compartment (endosome/lysosome, cytosol, and nucleus, $S_{(k)}$) was calculated. The fraction of pDNA in each compartment to the whole cell is calculated as: $F_{(k)}$ (%) = $S_{(k)}/S_{(tot)} \times 100$. See: Akita, H.; Ito, R.; Khalil, I. A.; Futaki, S.; Harashima, H. *Mol. Ther.* **2004**, *9*, 443−451.

JA055868+